Raman Spectroscopy of $(Ba_{1-x}Sr_x)(Mg_{1/3}Nb_{2/3})O_3$ Solid Solutions from Microwave-Hydrothermal Powders

Anderson Dias,*,† Franklin M. Matinaga,‡ and Roberto L. Moreira‡

Departamento de Química, Universidade Federal de Ouro Preto, Morro do Cruzeiro, Ouro Preto-MG, 35400-000, Brazil, and Departamento de Física, ICEx - Universidade Federal de Minas Gerais, C.P. 702, Belo Horizonte-MG, 30123-970, Brazil

Received December 18, 2006. Revised Manuscript Received March 2, 2007

Microwave-hydrothermal synthesis was employed to produce crystalline, single-phase $Ba(Mg_{1/3}Nb_{2/3})O_3$ and $Sr(Mg_{1/3}Nb_{2/3})O_3$ powders for the first time. The ceramics were mixed and fired at high temperatures to achieve ordered solid solutions. X-ray diffraction and Raman spectroscopy were employed to evaluate the crystal structure and phonon modes of chemically substituted $(Ba_{1-x}Sr_x)(Mg_{1/3}Nb_{2/3})O_3$ ($x = 0.0$, 0.3, 0.5, 0.7, 0.9, 1.0) microwave ceramics. It was verified that these materials present a phase transition for Sr-rich samples ($x \geq 0.7$), from trigonal D_{3d}^3 to monoclinic C_{2h}^3. Lorentzian lines were used to fit the spectra obtained at low temperatures, which present 35 bands for the $Sr(Mg_{1/3}Nb_{2/3})O_3$ ceramic. The position and width of the phonon modes were determined and correlated to the ionic radii, mass, and tolerance factors for the different atoms substituted in the A-site.

Introduction

In the last two decades, cellular base station technologies proliferated, and dielectric ceramics have known an increasing commercial importance as microwave materials for resonators and filters.[1] Despite their technological importance and widespread use, very few ceramic materials meet the property requirements imposed by the operating frequency, power levels, and type of applications (base station or handheld device).[2] Complex perovskites of the type $Ba(Zn_{1/3}Ta_{2/3})O_3$ constitute the only commercially available ceramic for frequencies in the gigahertz range.[1,2] The high costs associated with tantalum oxide changed the focus to cheaper niobium materials.[3] For these ceramics, it is well-known that processing conditions influence directly extrinsic factors like microstructure, defects, and porosity, which limit the frequency selectivity.[4] Besides, as pointed out by Reaney and Iddles,[2] in the 21st century, environmental considerations are becoming increasingly important. Thus, microwave ceramics must be processed in environmentally friendly conditions and should be recyclable.

Among the methods with high technological potential to prepare materials in mild conditions, the hydrothermal process is able to obtain nanostructured, crystalline powders in a single step.[5,6] Moreover, the use of microwave heating of the hydrothermal solutions enhances the kinetics of crystallization, allowing the production of electroceramics in relatively shorter times.[6] Also, previous papers[7,8] showed that the hydrothermal method produces materials with high long-range order parameters, which are critical for minimum dielectric losses. In this work, complex $(Ba,Sr)(Mg_{1/3}Nb_{2/3})O_3$ ceramics were synthesized by the microwave-hydrothermal method. For Sr-based perovskites, the method was applied for the first time, and the results are compared with those obtained for Ba-based materials in a previous publication.[6]

From an engineering perspective, the premise used to obtain a temperature-stable material (a very important microwave property) appears in a simple way: a solid solution is created between two materials with opposite signals of τ_e, the temperature coefficient of the dielectric constant. $Ba(Mg_{1/3}Nb_{2/3})O_3$ (BMN, with negative τ_e) and $Sr(Mg_{1/3}Nb_{2/3})O_3$ (SMN, with positive τ_e) powders were mixed in different stoichiometric proportions and sintered at high temperatures. Single-phase, highly ordered solid solutions with composition $(Ba_{1-x}Sr_x)(Mg_{1/3}Nb_{2/3})O_3$ ($x = 0.0$, 0.3, 0.5, 0.7, 0.9, 1.0) were obtained. For these mixed materials, the crystal structures have not been determined yet. Raman scattering is currently a powerful tool to investigate crystal structures of solid solutions through variations in the optical phonons, allowing also a correlation with the dielectric response in the microwave region.[9,10] Previous works have been devoted to studying the dielectric behavior of complex perovskites based on their phonon characteristics, whose knowledge helped the authors to understand the dielectric response of the systems.[10,11] In this

* Corresponding author. Tel.: +55-31-3559-1707. E-mail: anderson_dias@iceb.ufop.br.
† Universidade Federal de Ouro Preto.
‡ Universidade Federal de Minas Gerais.

(1) Vanderah, T. A. *Science* **2002**, *298*, 1182.
(2) Reaney, I. M.; Iddles, D. M. *J. Am. Ceram. Soc.* **2006**, *89*, 2063.
(3) Hughes, H.; Iddles, D. M.; Reaney, I. M. *Appl. Phys. Lett.* **2001**, *79*, 2952.
(4) Wersing, W. *Curr. Opin. Solid State Mater. Sci.* **1996**, *1*, 715.
(5) Feng, S.; Xu, R. *Acc. Chem. Res.* **2001**, *34*, 239.
(6) Dias, A.; Ciminelli, V. S. T. *Chem. Mater.* **2003**, *15*, 1344.
(7) Moreira, R. L.; Matinaga, F. M.; Dias, A. *Appl. Phys. Lett.* **2001**, *78*, 428.
(8) Dias, A.; Moreira, R. L. *J. Appl. Phys.* **2003**, *94*, 3414.
(9) Ratheesh, R.; Wöhlecke, M.; Berge, B.; Wahlbrink, Th.; Haeuseler, H.; Rühl, E.; Blachnik, R.; Balan, P.; Santha, N.; Sebastian, M. T. *J. Appl. Phys.* **2000**, *88*, 2813.
(10) Dias, A.; Khalam, L. A.; Sebastian, M. T.; Paschoal, C. W. A.; Moreira, R. L. *Chem. Mater.* **2006**, *18*, 214.

10.1021/cm0630035 CCC: $37.00
Published on Web 04/04/2007

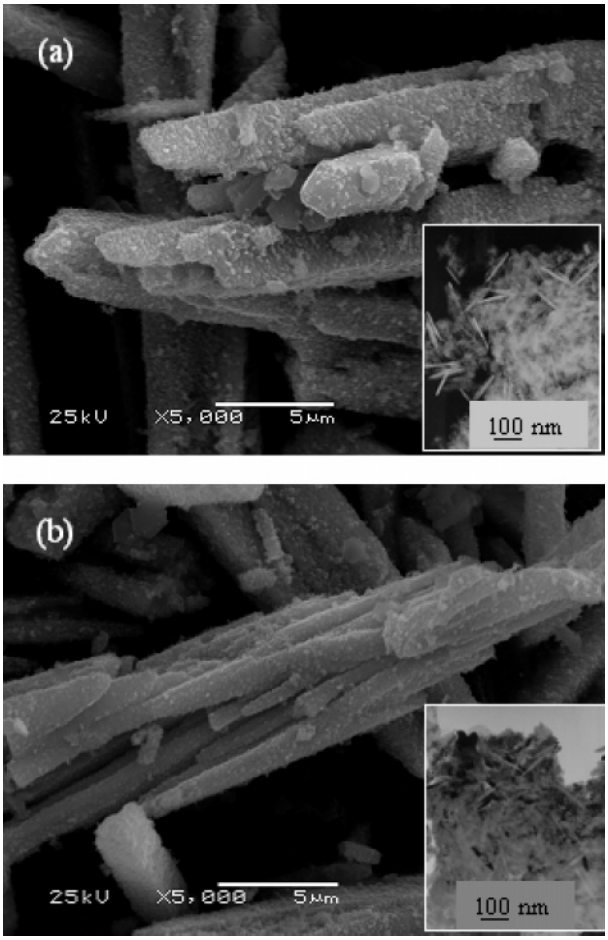

Figure 1. SEM and TEM (insets) images of the microwave-hydrothermal powders: (a) BMN and (b) SMN.

paper, Raman vibrational spectroscopy is employed to determine and assign the phonon modes (frequencies and full width at half-maximum) of $(Ba_{1-x}Sr_x)(Mg_{1/3}Nb_{2/3})O_3$ solid solutions from microwave-hydrothermal powders. Factor-group analyses are employed to predict the structural features of the materials. Raman spectra were obtained from room temperature (300 K) down to 30 K, and the results are discussed in terms of the structural changes caused by chemical substitution on the A-site, which can also be correlated to X-ray diffraction (XRD) data.

Experimental Section

$BaCl_2 \cdot 2H_2O$, $SrCl_2 \cdot 6H_2O$, and $MgCl_2 \cdot 6H_2O$ (>99%, Fluka Chemie AG, Switzerland), as well as $NH_4H_2[NbO(C_2O_4)_3] \cdot 3H_2O$ (>99%, CBMM, Brazil), were used as reagents to synthesize BMN and SMN. The salts were dissolved separately in deionized water (18.2 MΩ·cm) and mixed under stirring. The niobium ammonium oxalate was previously treated with a NaOH solution maintained at pH > 13 and washed to remove ammonia. After mixing, the precipitation occurred and the pH was controlled and adjusted to 13.5. BMN and SMN were synthesized separately by the microwave-hydrothermal process. A Milestone MLS-1200 MEGA microwave digestion system (2.45 GHz) was employed, according to procedures described in a previous paper.[6] Both compounds were produced under microwaves at 200 °C, for 2 h, and the resulting powders were repeatedly washed with deionized water and dried at 80 °C. Solid solutions between BMN and SMN were produced by mixing different amounts of the two ceramics to obtain a full range of compositions $(Ba_{1-x}Sr_x)(Mg_{1/3}Nb_{2/3})O_3$ ($x = 0.0, 0.3, 0.5, 0.7, 0.9, 1.0$). The samples were uniaxially pressed at 110 MPa and sintered in air at 1400 °C, for 4 h.

Structural analyses were carried out in a Philips PW1710 diffractometer with graphite monochromated and Ni filtered Cu Kα radiation (40 kV, 30 mA), in the 3−100° 2θ range (0.02° 2θ step size and 1 s/step). Transmission and scanning electron microscopes (Philips FEI-CM200 and JEOL 5410) were employed to study the morphological features of the BMN and SMN powders after processing. Micro-Raman scattering spectra were collected at room temperature using a triple-monochromator Jobin Yvon T64000 spectrometer, equipped with a liquid-N_2-cooled charge-coupled-device detector and an Olympus BXL microscope (100× and 20× objectives). The measurements were done in back-scattering geometry using the 532 nm line (second harmonic line from Nd:YVO_4 laser) as the excitation source (10 mW). The accumulation times were typically 10 collections of 5 s, and the spectral resolution was better than 2 cm^{-1}. Low-temperature measurements were conducted from 30 to 300 K in a controlled (Lakeshore) cold finger cryostat (Janis), with an accuracy of about 0.1 K. The resulting spectra were corrected by the Bose−Einstein thermal factor.

Results and Discussion

Microwave-hydrothermal processing produced crystalline, single-phase powders. Figure 1 presents SEM images of BMN (Figure 1a) and SMN (Figure 1b), which show large needle-like ceramics. TEM analysis (insets in Figure 1) showed that these needles are formed by nanostructured particles. The mean values for the width, length, and aspect ratio of the large needles are ∼2 μm, ∼50 μm, and 25, respectively. For nanosized particles, the same values can apply, but 3 orders of magnitude lower: 50 and 2 nm for length and width, respectively. These results show that the microwave-hydrothermal processing introduces a high anisotropy (with large aspect ratio) and a growing mechanism not previously observed in conventional autoclave processing of complex perovskites. Also, each large needle has a nearly uniform shape along its entire length, indicating that the growth anisotropy in the *c*-axis is strictly maintained throughout the process. As it can be seen in Figure 1, all separated materials show well-faceted crystal ends along the *c*-axis without branching. The microwave synthesis was successfully applied for the production of highly anisotropic particles of gold,[12] large aluminum phosphate crystals,[13] and hydroxyapatites.[14] However, the results presented here cannot be explained on the basis of these papers, particularly the production of large materials through "linking" of small particles.

Reduction in surface energy is the primary driving force for crystal growth and morphology evolution. In the present work, the phenomenon that links BMN and SMN needles

(11) Chia, C. T.; Chen, Y. C.; Cheng, H. F.; Lin, I. N. *J. Appl. Phys.* **2003**, *94*, 3360.

(12) Liu, F. K.; Chang, Y. C.; Ko, F. H.; Chu, T. C. *Mater. Lett.* **2004**, *58*, 373.

(13) Girnus, I.; Jancke, K.; Vetter, R.; Richter-Mendau, J.; Caro, J. *Zeolites* **1995**, *15*, 33.

(14) Siddharthan, A.; Seshadri, S. K.; Sampath Kumar, T. S. *Scr. Mater.* **2006**, *55*, 175.

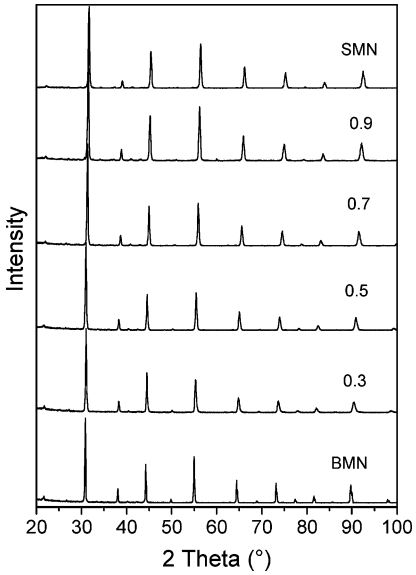

Figure 2. XRD patterns for the $(1 - x)$BMN−xSMN solid solutions sintered at 1400 °C, for 4 h. The values of x are indicated in the figure.

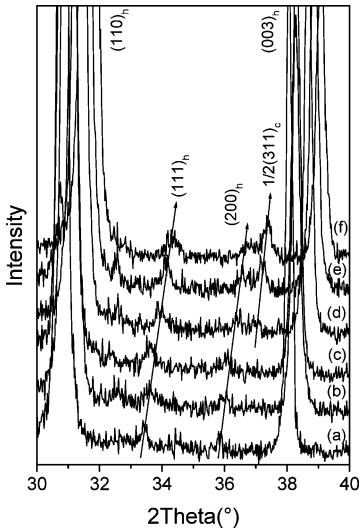

Figure 3. XRD patterns for the $(1 - x)$BMN−xSMN solid solutions in the 2θ range 30−40°. (a) $x = 0.0$; (b) $x = 0.3$; (c) $x = 0.5$; (d) $x = 0.7$; (e) $x = 0.9$; and (f) $x = 1.0$.

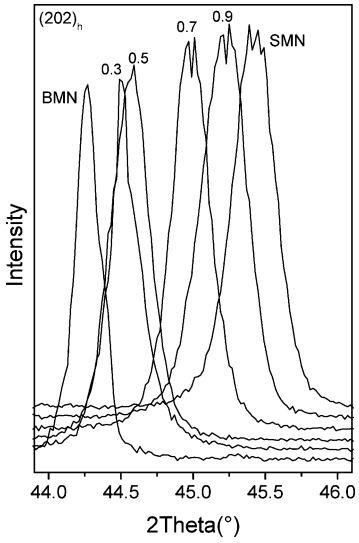

Figure 4. XRD patterns for the $(1 - x)$BMN−xSMN solid solutions in the 2θ range 44−46°. The values of x are indicated in the figure.

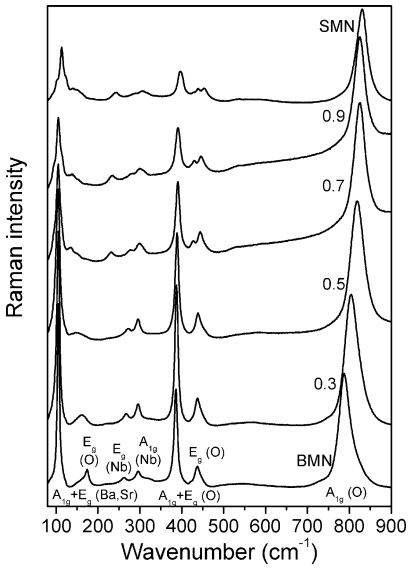

Figure 5. Raman spectra for all solid solutions of the ceramic system BMN−SMN. The assignments for the phonon modes in the trigonal phase are indicated in the figure.

could not be explained by the most cited Ostwald ripening process, in which crystal growth is described in terms of growth of larger particles at the expense of the smaller ones.[15] Microwaves have the useful property of heating some materials, while leaving others cold.[16,17] Essentially a high-frequency electric field, microwaves cause free ions or electrons to move in the same direction as the applied field. Under these conditions, the solvents (water in our case) become superheated and the precipitation (nucleation) occurs rapidly. This fast nucleation leads to the production of very fine particles, which are now free to move according to the applied electromagnetic fields in the microwave oven. In a second step, the nanostructured particles could undergo a multiplying growth via a "cementing mechanism". Thus, large crystals could be prepared from a direct combination of small crystals, which is also called "oriented attachment".[18−20] Under a microwave-hydrothermal condition, the side crystal planes are able to glue together to form larger crystals. This mechanism involves crystal growth by precise, crystallographically controlled addition of primary individual particles.[21] For the samples studied in the present work, the presence of OH^- ions in the strong alkaline aqueous solutions could favor oriented attachment under microwaves, allowing an intimate contact between the surface planes.

After microwave-hydrothermal synthesis, the powders were sintered at 1400 °C, for 4 h. XRD patterns for the mixed system $(Ba_{1-x}Sr_x)(Mg_{1/3}Nb_{2/3})O_3$ ($x = 0.0$, 0.3, 0.5, 0.7, 0.9, and 1.0) are presented in Figure 2. For this ceramic system,

(15) Baldan, A. *J. Mater. Sci*. **2002**, *37*, 2171.
(16) Adam, D. *Nature* **2003**, *421*, 571.
(17) Bergese, P. *Acta Mater.* **2006**, *54*, 1843.
(18) Zhang, H. Z.; Banfield, J. F. *Chem. Mater.* **2002**, *14*, 4145.
(19) Pacholski, C.; Kornowski, A.; Weller, H. *Angew. Chem., Int. Ed.* **2002**, *41*, 1188.
(20) Sampanthar, J. T.; Zeng, H. C. *J. Am. Chem. Soc*. **2002**, *124*, 6668.
(21) Hu, X. L.; Zhu, Y. J.; Wang, S. W. *Mater. Chem. Phys*. **2004**, *88*, 421.

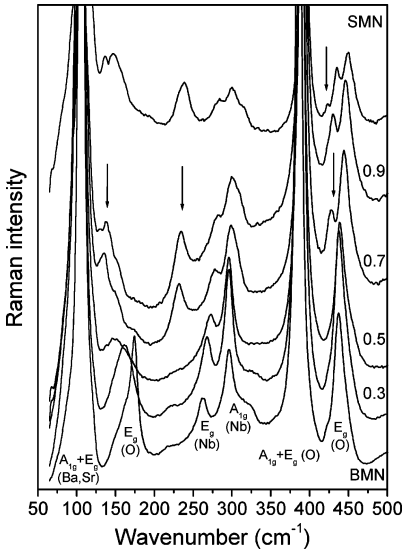

Figure 6. Raman spectra for the samples in the range 50−500 cm^{-1}. New bands for Sr-rich samples ($x \geq 0.7$) are indicated by arrows.

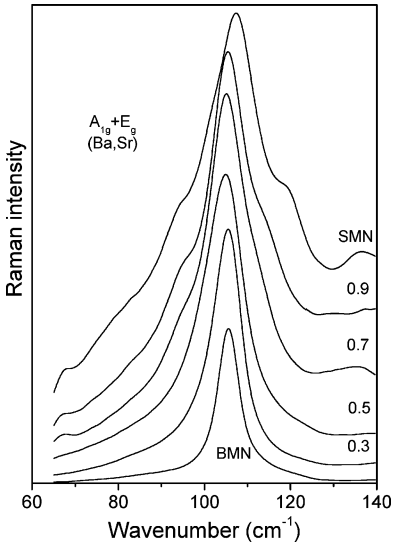

Figure 7. Frequency evolution for the ($A_{1g} \oplus E_g$) bands as a function of Sr content in the BMN−SMN system.

single-phase solid solutions were formed in the full-range composition. Pure BMN and SMN were indexed with ICDD card nos. 17-0173 and 17-0181, respectively. As a general trend, very narrow, intense diffraction peaks can be visualized, and no impurities or secondary phases were detected. Also, the peaks shifted to lower *d*-spacing for increasing strontium content. This behavior was expected, because Sr has a lower ionic radius if compared with Ba, decreasing the volume of the average unit cell. The most significant shift occurred between $x = 0.5$ and $x = 0.7$. Detailed analysis of the XRD data was carried out, and an extra peak could be identified besides a peak splitting in compositions with $x \geq 0.7$ (Sr-rich samples). The end members of the system $(Ba_{1-x}Sr_x)(Mg_{1/3}Nb_{2/3})O_3$ could be assumed as presenting a 1:2 ordered structure.[7,8,22,23] However, based on the results of Lee et al.,[22,23] a more careful analysis must be done in two 2θ regions of the XRD patterns: the first one at 30−40° 2θ and the second one at 44−46° 2θ.

Figure 3 presents the XRD patterns for the BMN−SMN system in the region 30−40° 2θ. The analysis was based on the nomenclature adopted by Lee et al.[22,23] and Nagai et al.[24] for a hexagonal cell of a $Ba(Sr_{1/3}Ta_{2/3})O_3$-type structure. Figure 3 shows the indexed peaks for a hexagonal cell and an extra peak at $2\theta \approx 37.3°$ for $x \geq 0.7$. This peak becomes more intense and shifts to lower *d*-spacing for higher values of *x*, being indexed as $1/2(113)_c$, based on the simple cubic perovskite unit cell.[24] According to Lee et al.[22,23] and Nagai et al.,[24] the antiphase tilting of the oxygen octahedra would be responsible for its appearance (odd−odd−odd reflections). Figure 4 shows that the $(202)_h$ peak shifts to higher 2θ angles and also splits for $x \geq 0.7$. Nagai et al.[25] identified these peaks only for $x \geq 0.9$ and indexed them successfully as $2\bar{4}2$ and 242 peaks in terms of their monoclinic phase, which has antiphase tilting of the oxygen octahedra. According to these authors, the space group of the structure changed from D_{3d}^3 (trigonal) to C_{2h}^6 (monoclinic), which is a doubled unit cell along the *c*-axis of the hexagonal cell. According to Lee et al.,[22,23] the splitting of the $(202)_h$ peak implies that SMN and the solid solutions with $x \geq 0.7$ have a distorted 1:2 ordered structure rather than the normal structure of BMN, supporting the hypothesis that the distortion of the unit cell was caused by oxygen tilting.

In view of the discrepancies observed in the X-ray data, Raman spectroscopic analysis was conducted in all samples of the system BMN−SMN to clarify the structural changes observed by XRD. Lee et al.[22,23] also studied the microstructure and dielectric properties of BMN−SMN solid solutions as a function of the tolerance factor and identified two regions: for compositions with $x \leq 0.5$, the ceramics are 1:2 ordered trigonal structure without tilting of oxygen octahedra; for compositions with $0.7 \leq x \leq 1.0$, the materials maintain the 1:2 chemical ordering but introduce an antiphase tilting of oxygen octahedra. Much evidence was discussed, including a significant variation of temperature coefficient of dielectric permittivity (τ_e), from −50.5 ppm/°C in pure BMN to +8.0 ppm/°C in pure SMN. For $x = 0.5$ (tolerance factor nearly the unity), τ_e reaches a minimum value of −150 ppm/°C in the borderline between untilted and antiphase tilted octahedra. Tolerance factor (*t*) values higher than the unity correspond to large spaces for *B*-ion vibrations, while *t* smaller than the unity are related to large spaces for *A*-ion vibrations. In the present case, the Sr-ions are too small and the tilting of the oxygen octahedra takes place. Nagai et al.[25] studied an anomaly in the infrared-active phonon modes in Ba−Sr solid solutions with tantalum and verified the appearance and splitting of some phonon modes in tilted ceramics. Tilted transitions occur when corner-shared oxygen octahedra rotate either in phase or antiphase around the major axes of the perovskite structure. As in the paper of Nagai et al.,[25] similar results are expected for the niobate analogue system BMN−SMN.

(22) Lee, H. J.; Park, H. M.; Song, Y. W.; Cho, Y. K.; Nahm, S.; Byun, J. D. *J. Am. Ceram. Soc*. **2001**, *84*, 2105.
(23) Lee, H. J.; Park, H. M.; Song, Y. W.; Cho, Y. K.; Nahm, S.; Byun, J. D. *J. Am. Ceram. Soc*. **2001**, *84*, 3032.
(24) Nagai, T.; Sugiyama, M.; Sando, M.; Niihara, K. *Jpn. J. Appl. Phys*. **1997**, *36*, 1146.
(25) Nagai, T.; Sugiyama, M.; Sando, M.; Niihara, K. *Jpn. J. Appl. Phys*. **1996**, *35*, 5163.

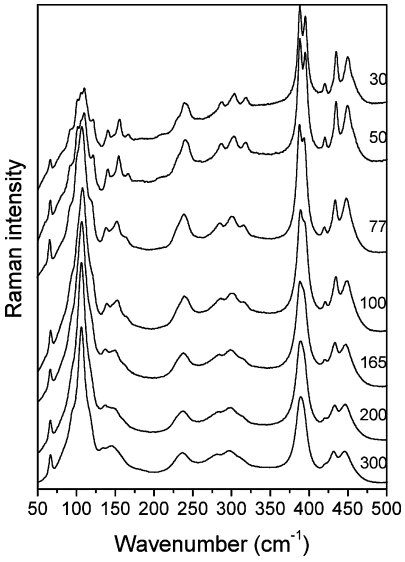

Figure 8. Low-temperature Raman spectra for the SMN samples. The temperatures are indicated in the figure.

Figure 5 presents the Raman spectra of all samples studied in the present work. For pure BMN, nine bands can be easily identified and assigned, accordingly to previous papers.[7,8,11] For BMN, two overlapping bands around 105 cm^{-1} are due to A_{1g} (Ba) and E_g (Ba) symmetry modes, while modes associated with oxygen ions occur at 386 and 788 cm^{-1} (A_{1g}) and 174, 386, and 437 cm^{-1} (E_g). Bands due to niobium ions occur at 263 cm^{-1} (E_g) and 296 cm^{-1} (A_{1g}). It is clear that the introduction of strontium promotes smooth changes in the spectra for $x \leq 0.5$ and more pronounced effects for $x > 0.5$. The A_{1g} (O) mode, assigned to the breathing of the oxygen octahedra,[7−11] presented a shift to higher frequencies from 788 cm^{-1} (pure BMN) to 830 cm^{-1} (pure SMN). This behavior is due to the high sensitivity of this phonon mode to the volume of the unit cell.[7−11] Other important changes with the introduction of Sr are in the frequency range 100−500 cm^{-1} and are explained below.

Figure 6 presents the Raman spectra of the samples in the range 50−500 cm^{-1} in detail. The peak profiles of the spectra for $x \leq 0.5$ are similar, except for the shifts observed toward higher frequencies, as explained above. The bands in the region 105−175 cm^{-1} shifted to lower frequencies (not expected) and represent a particular feature of these samples. This dependence of the frequencies on the change of the Sr content indicates that the phonon modes are sensitive to structure rather than to the mass of vibrating ions. For $x \geq 0.7$, numerous additional peaks appeared (at least four new modes can be visualized, as indicated by arrows in Figure 6), as also verified by Sugiyama and Nagai[26] in $(Ba_{1-x}Sr_x)(Mg_{1/3}Ta_{2/3})O_3$ solid solutions. It is suggested from Raman spectroscopy that the crystal structure of the ceramics with $x \geq 0.7$ is of lower symmetry in comparison with the trigonal BMN symmetry. One of the possible reasons for the appearance of the additional phonon modes includes the effect of the distortion of the normal trigonal cell toward a monoclinic phase (C_{2h}^6 according to Nagai et al.[24]), with antiphase tilting of the oxygen octahedra. The additional bands would occurr as a consequence of the splitting of the A_{1g} and E_g phonon modes at 105 cm^{-1} (BMN), giving rise to the 94.6 and 119 cm^{-1}, besides new intense bands at 136.3, 237.6, and 423.4 cm^{-1} (positions for pure SMN). The exact number of bands in the samples with lower symmetry ($x \geq 0.7$) will be determined after peak deconvolution.

Figure 7 shows the lowest frequency (trigonal $A_{1g} \oplus E_g$) modes for the BMN−SMN solid solution studied here. These bands are due to the lattice vibrations of Ba and Sr ions, and it is clear that the replacement of bigger Ba ions by smaller Sr ions has appreciable influence over the volume reduction and the bonding character between A−O and B−O ions. For these bands, an interesting behavior could be detected: samples with $x \leq 0.5$ present a good symmetric peak (only one Lorentzian line) that shifts to lower frequencies for increasing x, while samples with $x \geq 0.7$ exhibit at least three peaks shifting to higher frequencies. This behavior was previously observed by Venkatesh et al.[27] in polar phonon modes of $(Ba_{1-x}Sr_x)(Zn_{1/3}Ta_{2/3})O_3$ solid solutions and by Youn et al.[28] in lanthanum-barium magnesium niobate ceramics. For the first group of ceramics ($x \leq 0.5$, untilted structures), substitution of Sr ions would reduce the overlapping of A and O ions and hence a decrease of force constant between A−O ions is expected.[27] It is worthy noticing the broadening of the lowest frequency peak, compatible with the necessary disorder of Ba and Sr ions in the A-site of the trigonal structure. For the second group of materials ($x \geq 0.7$), a tilted structure occurs with a further reduction in the A-site coordination number (from 12 in untilted to 8 in tilted structures) and, consequently, an increase in overlapping of A and O ions. Thus, an increase in the force constant for the vibration involving A and O ions occurs.[27] Because the B-site ions are kept constant (Mg and Nb) for all the solid solutions, the volume reduction may be associated with decrease in the bond length of B−O ions with increasing Sr ion concentration at the A-sites. This would increase the covalency between B and O ions, and, hence, the associated force constant of the vibrating mode should also increase, correspondingly.

The structural change verified with the introduction of Sr ions in Ba-based magnesium niobates was evaluated by Raman spectroscopy from room temperature down to 30 K. The spectrum for SMN represents the final distorted structure and was studied in detail. Lorentzian lines were employed to fit (after Bose−Einstein correction) and, therefore, to determine the number of phonon modes for this sample. The hypothesis for SMN sample includes the assumption of a distorted, tilted perovskite with tolerance factor around 0.97 (antiphase tilting). According to Howard and Stokes,[29] perovskites of the $A_3BB'_2O_9$-type present 1:2 B-site cation ordering and, in the absence of octahedral tilting, belong to the parent structure $P\bar{3}m1$ space-group symmetry. The authors used group theory tools to show that nine different structures are possible as a consequence of lowering sym-

(26) Sugiyama, M.; Nagai, T. *Jpn. J. Appl. Phys*. **1993**, *32*, 4360.
(27) Venkatesh, J.; Subramanian, V.; Murthy, V. R. K. *Physica B* **2000**, *293*, 118.
(28) Youn, H. J.; Hong, K. S.; Kim, H.; Kim, H. *J. Korean Phys. Soc*. **1998**, *32*, S524.
(29) Howard, C. J.; Stokes, H. T. *Acta Crystallogr*. **2004**, *B60*, 674.

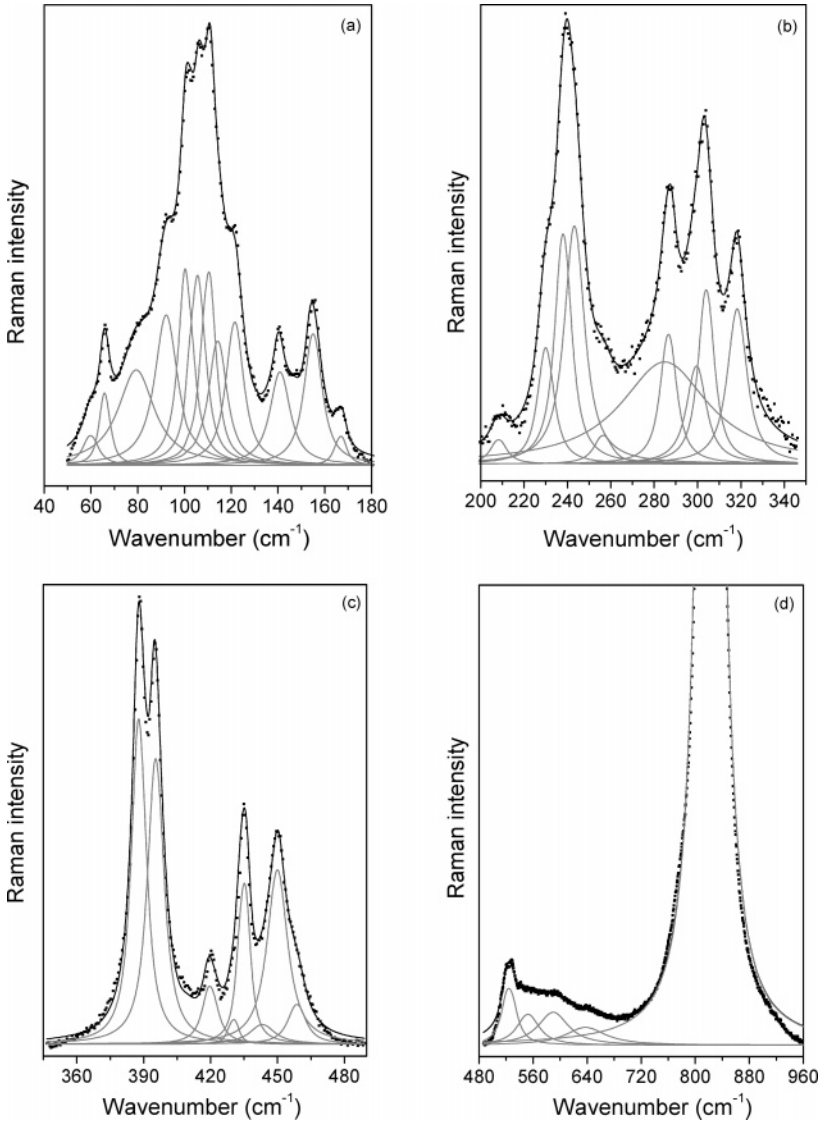

Figure 9. Raman spectrum for SMN microwave ceramic at 30 K. The experimental data (solid squares) were fitted (black line) with a sum of 35 (total) Lorentzian curves (gray lines). (a) 40−180 cm^{-1}; (b) 300−350 cm^{-1}; (c) 350−480 cm^{-1}; and (d) 480−960 cm^{-1}.

metry by octahedral tilting. The group−subgroup relationships were obtained and are used in the present work to describe the phase transition in the $(Ba_{1-x}Sr_x)(Mg_{1/3}Nb_{2/3})O_3$ system. Starting from the space group $P\bar{3}m1$ (trigonal, untilted), the derived subgroups in our case would be $P\bar{3}$, $C2/m$, $P2_1/c$, $A2/m$, and $P\bar{3}c1$.[29] Among the five subgroups listed above, only the space groups $A2/m$ and $P\bar{3}c1$ contain antiphase tilting. The space group $P\bar{3}c1$ presents antiphase tilting in all the three axes ($a^-a^-a^-$, according to Glazer notation) and probably does not apply for SMN samples. Thus, the only possible monoclinic structure derived from antiphase tilting of the oxygen octahedra is the space group $A2/m$ (or C_{2h}^3, No. 12), which includes two tilts $a^0b^-b^-$. This conclusion does not agree with the structure proposed by Nagai et al.[24] for a monoclinic $C2/c$ or $A2/n$ (C_{2h}^6). According to Howard and Stokes,[29] this structure is derived from $P\bar{3}c1$ space group, and the phase transition between them is required by Landau theory to be of first order.[30]

The assumed structure for SMN ceramics ($A2/m$, C_{2h}^3) presents a direct relationship with the untilted $P\bar{3}m1$ space group, from trigonal to monoclinic with antiphase tilting of the oxygen octahedra. For a factor-group analysis, the atomic positions must be considered and Wyckoff symbols for SMN (here considered as $Sr_3MgNb_2O_9$) are as follows: the Sr atoms occupy three 4*i* sites of special C_s symmetry, Mg ions are on 2*a* and 2*d* positions (C_{2h} symmetry), Nb ions occupy two 4*i* sites, and the oxygen atoms are in three 8*j* and three 4*i* sites (C_1 and C_s symmetries, respectively). Then, using the site-group method of Rousseau et al.[31] it is possible to obtain the Raman active phonon modes at the Brillouin zone center for this C_{2h} point group: $\Gamma_R = 25A_g \oplus 17B_g$. Thus, 42 Raman bands ($A_g$, B_g) are expected for this group. Figure 8 presents the spectra for the SMN samples obtained at 30, 50, 77, 100, 165, 200, and 300 K. As it can be observed, the spectrum at 300 K presents at least 18 bands, which is a small number if compared with the theoretical predictions

(30) Landau, L. D.; Lifshitz, E. M. *Statistical Physics*, 3rd ed.; Pergamon Press: New York, 1980; Chapter XIV.

(31) Rousseau, D. L.; Bauman, R. P.; Porto, S. P. S. *J. Raman Spectrosc.* **1981**, *10*, 253.

Table 1. Phonon Modes Parameters (Frequency and Full Width at Half-Maximum) from Raman Analysis at 30 K for the SMN Sample[a]

band	frequency (cm^{-1})	fwhm (cm^{-1})	α (10^{-3} cm^{-1}/K)
1	59.9	6.7	−36
2	65.9	4.2	−22
3	79.4	18.2	−24
4	92.2	10.8	−28
5	100.7	6.7	−20
6	105.8	6.8	−52
7	110.3	6.1	−50
8	114.2	8.4	−66
9	121.5	8.1	−20
10	140.9	9.4	−40
11	155.0	8.1	−48
12	166.8	4.5	−16
13	208.3	7.6	−36
14	230.1	7.7	−42
15	238.1	7.9	−104
16	243.2	10.1	−66
17	256.5	8.8	−66
18	284.9	48.6	−76
19	286.6	7.6	−10
20	299.5	9.8	−108
21	304.1	7.5	−64
22	318.3	9.7	−36
23	387.8	6.8	−106
24	395.4	7.6	−18
25	419.8	7.0	−110
26	430.2	3.6	−78
27	435.0	4.8	−22
28	443.2	12.8	−40
29	450.0	10.0	−28
30	458.7	8.5	−30
31	524.4	20.1	−50
32	552.4	35.6	−32
33	589.7	51.3	−88
34	637.7	69.5	−30
35	822.3	28.1	−68

[a] α is the temperature derivative of the phonon position.

and, thus, not appropriate to obtain the correct structure. The sample was cooled down to 30 K, and the number of bands increased significantly. This behavior was not due to additional phase transition, and the phonon modes that overlapped in higher temperatures could now be easily identified. As a general trend, the cooling of the sample produced harder modes, which shifted to higher vibrational frequencies as the temperature decreased from 300 to 30 K. Also, a strong luminescence background appeared upon cooling and becomes greater and greater down to 30 K. This background was removed before fitting.

The spectrum obtained at 30 K represents the best data set for the study of the structure of the SMN sample. Figure 9 shows the experimental data (solid squares) fitted (black line) by a sum of Lorentzian lines (gray lines) after removal of the background due to luminescence. The spectrum was divided into four regions (Figures 9a−d) to facilitate visualization and analysis due to the high number of bands. Deconvolution of the spectrum identified 35 bands for a total of 42 phonon modes expected by the factor-group analysis. A higher number of Lorentzian lines could be used in the fitting procedure. However, this procedure does not look appropriated, because accidental quasi degeneracy between modes belonging to the different A_g and B_g irreductible representations (i.r.) are quite probable in this system, which cannot be resolved with unpolarized spectra of non-oriented ceramics. Table 1 shows the fitting parameters (phonon frequencies, full width at half-maximum, and the linear temperature coefficient of frequency variation, α) obtained from Figure 9. The higher number of phonon modes was identified in the spectrum region 50−180 cm^{-1} (12 bands), followed by the region 200−350 cm^{-1} (10 bands). The region 350−500 cm^{-1} of the spectrum showed 8 bands, while the region 500−900 cm^{-1} exhibited only 5 bands. We remark that, although the mode nos. 18 and 19 (Table 1) are very close (superimposed), no coupling between them was observed (symmetric band profiles), probably because they belong to different i.r. The number of depicted modes was very close to the theoretical predictions, although the complete assignment for this low-symmetry SMN sample could not be accomplished. It is believed that the assumption for a monoclinic $A2/m$, C_{2h}^3, structure is the correct one for this tilted microwave material. The negative sign of α for all modes shows normal phonon behavior due to the lattice thermal expansion.

Finally, we notice that there are not excedent modes in the Raman spectra of the solid solutions, which means that although the unit cells cannot be strictly the same as in the pure systems, there would exist a pseudo-Brillouin zone that qualitatively varies little as the composition is changed (one for each phase, trigonal or monoclinic). This result is confirmed by XRD measurements and with the proposition of an average unit cell with D_{3d}^3 structure for $x \leq 0.5$ and a C_{2h}^3 structure for $x \geq 0.7$.

Conclusions

Microwave-hydrothermal synthesis was employed to produce crystalline, single-phase $Ba(Mg_{1/3}Nb_{2/3})O_3$ and $Sr(Mg_{1/3}Nb_{2/3})O_3$ powders for the first time. The ceramics were mixed and fired at high temperatures to achieve ordered solid solutions. XRD and low-temperature Raman spectroscopy were employed to evaluate the crystal structure and phonon modes of chemically substituted $(Ba_{1-x}Sr_x)(Mg_{1/3}Nb_{2/3})O_3$ ($x = 0.0$, 0.3, 0.5, 0.7, 0.9, 1.0) microwave ceramics. It was verified that these materials present a phase transition for Sr-rich samples ($x \geq 0.7$), from trigonal D_{3d}^3 to monoclinic C_{2h}^3. Lorentzian lines were used to fit the spectra, which present 35 bands at 30 K for the $Sr(Mg_{1/3}Nb_{2/3})O_3$ ceramic. The position and full-width at half-maximum of the phonon modes were determined and correlated to the ionic radii, mass, and tolerance factors for the different atoms substituted in the A-site.

Acknowledgment. The authors acknowledge the financial support from MCT/CNPq, FINEP, and FAPEMIG.

CM0630035